Dynamical Masses of Local Group Galaxies
Proceedings IAU Symposium No. 379, 2025
P. Bonifacio, M.-R. Cioni, F. Hammer, M. S. Pawlowski & S. Taibi, eds.
doi:10.1017/S1743921323001126

Low-mass galaxy rotation curves that fail as dynamical mass tracers

K. A. Oman[1,2] and E. R. Downing[1,2]

[1]Institute for Computational Cosmology, Durham University, South Road, Durham, DH1 3LE, United Kingdom
email: kyle.a.oman@durham.ac.uk

[2]Department of Physics, Durham University, South Road, Durham, DH1 3LE, United Kingdom

Abstract. It is routinely assumed that galaxy rotation curves are equal to their circular velocity curves (modulo some corrections) such that they are good dynamical mass tracers. We analysed 33 low-mass galaxies from the APOSTLE simulation suite to explore the limits of validity of this assumption. Only 3 galaxies have rotation curves similar to their circular velocity curves; the rest are undergoing a wide variety of dynamical perturbations. We assessed how many galaxies are likely to be strongly perturbed by processes in several categories: mergers/interactions, bulk gas flows, non-spherical DM halo, warps, and IGM ram pressure. Most galaxies fall into more than one of these categories; only 5/33 are not in any of them. The sum of these effects leads to an underestimation of the low-velocity slope of the baryonic Tully-Fisher relation that is difficult to avoid, and could contribute to the observed diversity in low-mass galaxy rotation curve shapes.

Keywords. Galaxy kinematics and dynamics, Dwarf galaxies, Dark matter

1. Introduction

The present contribution summarizes the content of the poster presented at IAU Symposium 379. A more detailed and complete account of the work presented is published in Downing & Oman (2023).

2. The APOSTLE simulations

The APOSTLE simulations (Sawala *et al.* 2016; Fattahi *et al.* 2016) are a suite of fully cosmological hydrodynamical zoom-in simulations of 12 volumes approximately 5 Mpc in diameter. The simulations used in this work have a mass resolution of about 10^4 $M_\odot$ (gas) or 10^5 $M_\odot$ (dark matter), with a minimum force softening of about 130 pc. The APOSTLE project uses an identical galaxy formation model as was used in the EAGLE simulation project, and the 'REFERENCE' model calibration (Schaye *et al.* 2015; Crain *et al.* 2015). APOSTLE galaxies are labelled with a unique identifier according to: their resolution level (in this work always the highest resolution 'L1' used in the project); the identifier of the volume from 1 to 12 (e.g. 'V6'); their group identifier composed of a friends-of-friends group identifier (indexed from 1) and a subhalo identifier (indexed from 1 – a value of 0 indicates a 'central' as opposed to a 'satellite' galaxy). Fig. 1 shows visualisations of the gas discs of the low-mass galaxies analysed in this work.

© The Author(s), 2025. Published by Cambridge University Press on behalf of International Astronomical Union.

https://doi.org/10.1017/S1743921323001126 Published online by Cambridge University Press

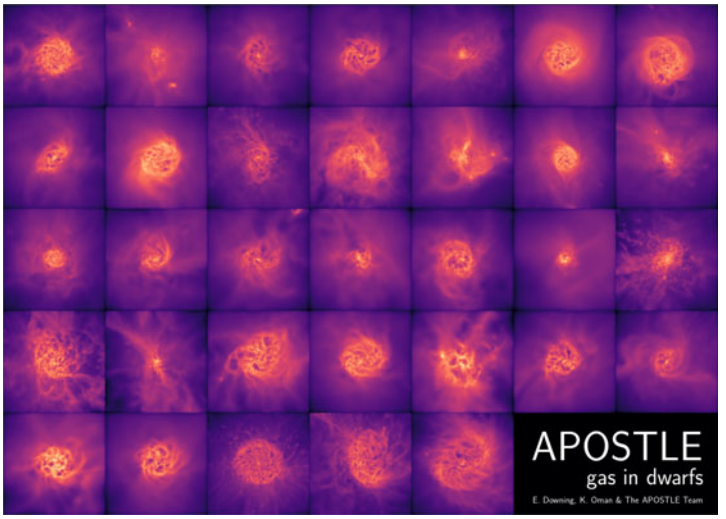


Figure 1. Gas discs at $z = 0$ seen face-on of the 33 low-mass ($60 < v_{\rm max}/{\rm km\,s^{-1}} < 120$) central (not satellite) galaxies from the highest-resolution APOSTLE simulation runs used in this work.

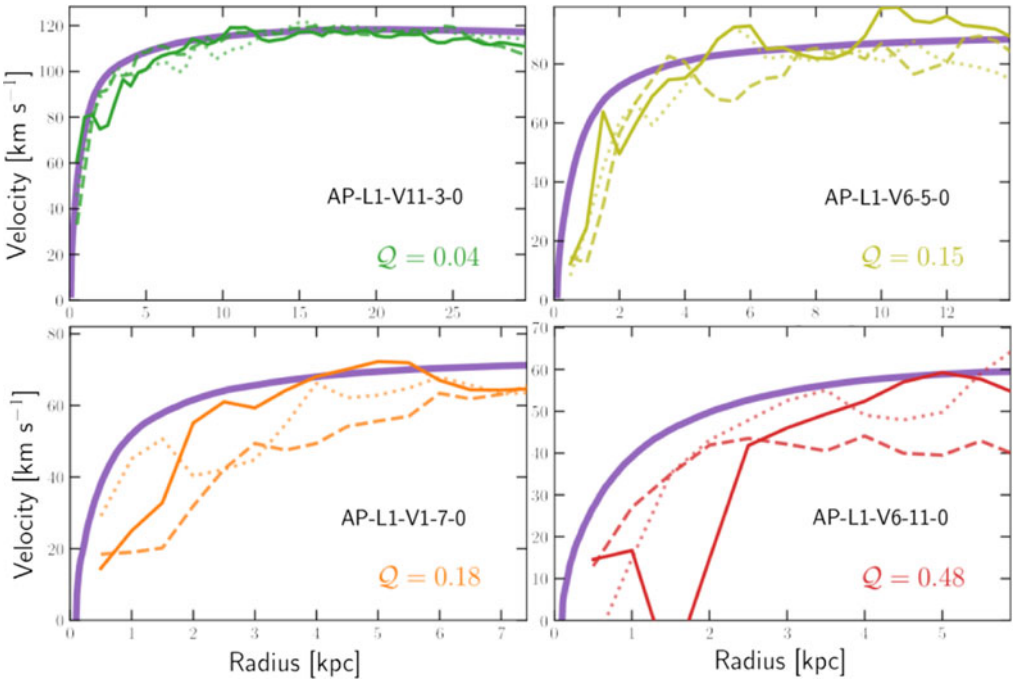


Figure 2. Rotation curves for 4 example galaxies at the end of the simulation (solid lines) and 300 and 600 Myr earlier (dashed and dotted lines). The heavy purple lines show the circular velocity curves at the end of the simulation (these evolve only very slowly).

3. Rotation curves and circular velocity curves

For every galaxy we calculated the orbital velocity expected from the potential: the circular velocity. We also measured the rotation curve (azimuthalvelocity of the gas)

https://doi.org/10.1017/S1743921323001126 Published online by Cambridge University Press

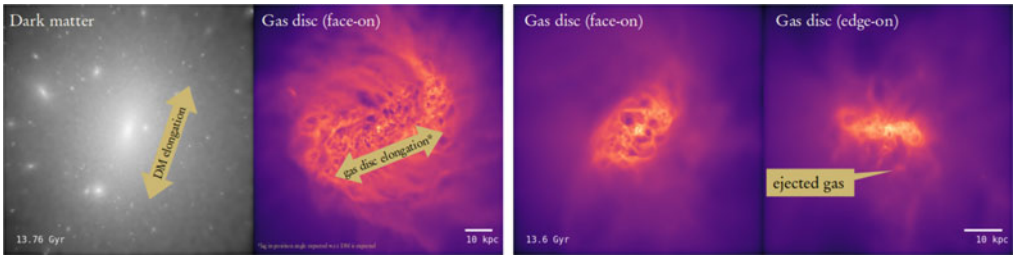


Figure 3. *Left panel pair:* Face-on view of the gas disc (right) and the dark matter (left, same perspective) of galaxy AP-L1-V11-6-0. The DM halo is visibly elongated, driving transient lopsided ($m = 1$ harmonic) and bisymmetric ($m = 2$) deformations of the gas disc. *Right panel pair:* Face-on (left) and edge-on (right) views of the gas disc of galaxy AP-L1-V4-13-0. Several prominent whisps of vertically ejected gas are visible both above and below the disc in the interval from about 13.0 – 13.8 Gyr.

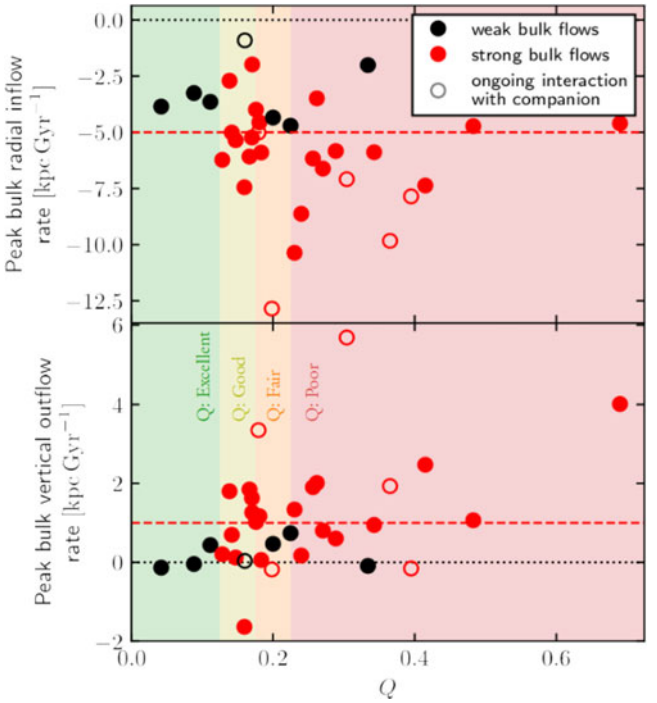


Figure 4. *Upper panel:* Anti-correlation between peak (cylindrical) radial flow rate in the last 600 Myr of the simulation and the degree to which the rotation curve traces the circular velocity curve, Q. *Lower panel:* Correlation between peak vertical (out)flow rate and Q. Points which exceed a threshold for 'strong' flows (dashed line) in either panel are coloured red.

at 300 Myr intervals. We defined a measure Q of the agreement between the rotation and circular velocity curves. A higher Q value indicates a rotation curve that is a poorer tracer of the circular velocity curve. We qualitatively classified galaxies as 'excellent'/'good'/'fair'/'poor' based on their Q. Fig. 2 shows one example from each of these categories. The lower-left panel illustrates that Q is penalized for discrepancies between the present-day rotation curve and circular velocity curve (over at least 25% of

https://doi.org/10.1017/S1743921323001126 Published online by Cambridge University Press

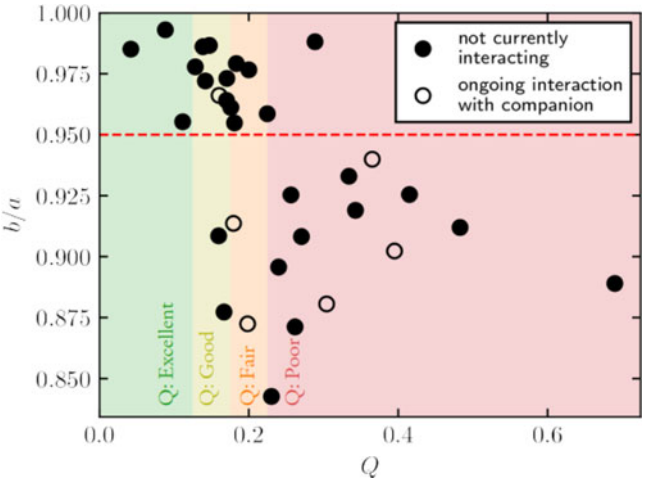


Figure 5. Anti-correlation between dark matter halo intermediate-to-major axis ratio b/a and the degree to which the rotation curve traces the circular velocity curve, Q.

its radial extent). The lower-right panel illustrates that Q is futher penalized for more time-variability in the rotation curve.

4. Kinematic perturbations

For each galaxy, we made several videos visualising the gas and dark matter. We visually identified many features linked to perturbations of the gas disc: mergers or interactions with companions; bulk gas flows (radial and/or vertical); elongation of the DM halo; gas disc warps; ram-pressure wind from the IGM. Our initial visual analysis guided a more quantitative follow-up analysis. Fig. 3 shows two examples drawn from our collection of visualisations. We elaborate briefly on two types of perturbations, as examples.

The strength of non-circular bulk gas flows in the disc (radial or vertical) correlates with Q (Fig. 4). Galaxies with strongly perturbed rotation curves tend to also have strong bulk gas flows.

DM halo intermediate-to-major axis ratio (b/a) anti-correlates with Q (Fig. 5). Even a mildly prolate or triaxial DM halo shape in the disc region ($b/a \lesssim 0.95$) can strongly perturb the gas.

5. Conclusions

Only about 30% (12/33) of galaxies in our sample have rotation curves that trace their circular velocity curves reasonably well, and only about 10% (3/33) are close matches. Causes include: mergers/interactions with companions (6/33); accretion-driven gas inflows (19/33); supernova-driven gas outflows (15/33); prolate/triaxial DM haloes (17/33); gas disc warps (8/33); and IGM ram pressure (5/33). Most galaxies fall in more than one category.

As a consequence, the baryonic Tully-Fisher relation (McGaugh 2000) and other kinematic scaling relations may suffer from severe biases, as illustrated in Fig. 6.

https://doi.org/10.1017/S1743921323001126 Published online by Cambridge University Press

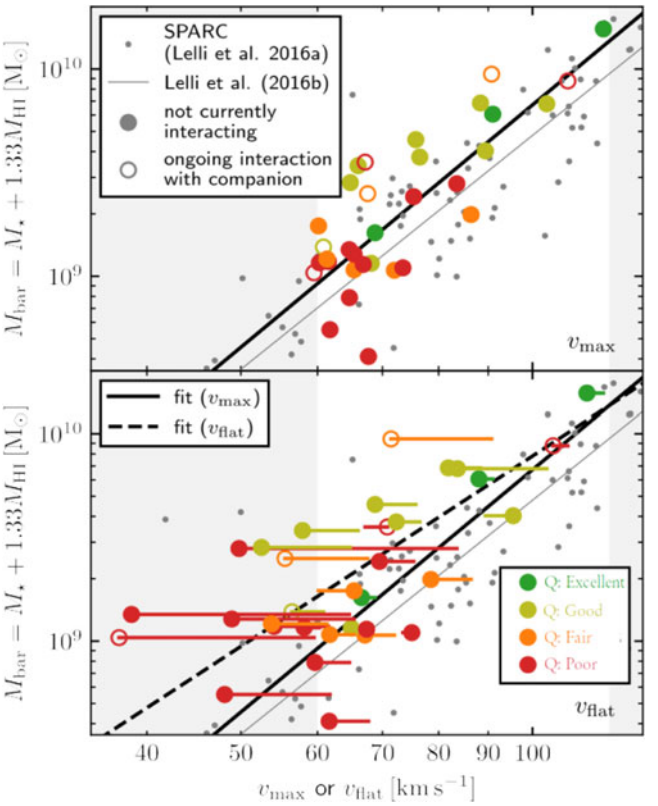


Figure 6. *Upper panel:* The baryonic Tully-Fisher relation (BTFR) for our sample of low-mass galaxies where $v_{\rm max}$ is calculated from their circular velocity curves – the 'true' BTFR. The heavy line is a fit to the filled coloured points. *Lower panel:* The BTFR for the same sample of galaxies, but where $v_{\rm flat}$ is measured from their rotation curves. The points are joined to their positions in the upper panel by horizontal line segments. The maximum gas rotation velocity ($v_{\rm flat}$) systematically underestimates the maximum circular velocity ($v_{\rm max}$), and the underestimates get systematically worse at lower $v_{\rm max}$; this has the potential to bias both the normalisation and slope of the BTFR, as illustrated by the dashed fit line.

Acknowledgements

KAO: European Research Council (ERC) Advanced Investigator grant to C.S. Frenk, DMIDAS (GA 786910), and STFC grant ST/T000244/1. ERD: a Durham Physics Developing Talent Award to KAO. This work used the DiRAC@Durham facility managed by the Institute for Computational Cosmology on behalf of the STFC DiRAC HPC Facility (www.dirac.ac.uk). The equipment was funded by BEIS capital funding via STFC capital grants ST/K00042X/1, ST/P002293/1, ST/R002371/1 and ST/S002502/1, Durham University and STFC operations grant ST/R000832/1. DiRAC is part of the National e-Infrastructure. Elements of this work, in particular Figs. 2, 4, 5 & 6, are adapted from Downing & Oman (2023) as permitted under the terms of that work's license (CC BY 4.0; https://creativecommons.org/licenses/by/4.0/).

References

Crain, R. A., Bahé, Y. M., Lagos, C. del P., *et al.* 2015, MNRAS, 450, 1937
Downing, E. R., Oman, K. A. 2023, MNRAS, in press.

https://doi.org/10.1017/S1743921323001126 Published online by Cambridge University Press

Fattahi, A., Navarro, J. F., Sawala, T., *et al.* 2016, MNRAS, 457, 844
McGaugh, S. S. 2000, ApJ, 533, L99
Sawala, T., Frenk, C. S., Fattahi, A., *et al.* 2016, MNRAS, 457, 1931
Schaye, J., Crain, R. A., Bower, R. G., *et al.* 2015, MNRAS, 446, 521

https://doi.org/10.1017/S1743921323001126 Published online by Cambridge University Press